Water Practice & Technology

IWA PUBLISHING

Water Practice & Technology Vol 17 No 1, 75 doi: 10.2166/wpt.2021.091

Chemical deposition of iron nanoparticles (Fe^0) on titanium nanowires for efficient adsorption of ciprofloxacin from water

Omar Falyouna[a,*], Ibrahim Maamoun[a], Khaoula Bensaida[a], Atsushi Tahara[b], Yuji Sugihara[a] and Osama Eljamal[a]

[a] Department of Earth System Science and Technology, Interdisciplinary Graduate School of Engineering Sciences, Kyushu University, 6-1 Kasuga-Koen, Kasuga, Fukuoka 816-8580, Japan
[b] Creative Interdisciplinary Research Division, Frontier Research Institute for Interdisciplinary Sciences (FRIS), Tohoku University, Sendai, Japan
*Corresponding author. E-mail: omar.falyouna@kyudai.jp

OE, 0000-0003-4052-6720

ABSTRACT

The development of antimicrobial resistance genes (AMRs) in water was globally accelerated due to the occurrence of ciprofloxacin (CIP) in water. This study aims to precipitate iron nanoparticles (Fe^0) on the surface of titanium nanowires (TNWs) through a chemical process to overcome the limitations of Fe^0 and efficiently remove CIP from water. TEM and XRD results confirmed the successful synthesis of Fe^0 and TNWs. They also proved the successful deposition and dispersion of Fe^0 on TNWs. Several (Fe^0/TNW) nanocomposites were synthesised with different percentages of TNWs (5, 10, 20, 30, and 50%) to define the best TNWs ratio that will decrease the aggregation of Fe^0 nanoparticles and achieve an outstanding removal efficiency of CIP. (Fe^0/TNW) nanocomposite with 20% of TNW was nominated as the best nanocomposite because it demonstrated a promising performance, compared with other nanocomposites, by removing more than 67% of CIP with insignificant desorption behaviour during the treatment period (120 min). Dosage of (20%-Fe^0/TNW), initial pH of CIP solution and reaction temperature were optimized through a group of batch experiments to efficiently remove CIP from water. The optimum removal of CIP was obtained by 1 g L^{-1} of (20%-Fe^0/TNW) nanocomposite at initial pH of 7 under 35 °C.

Key words: adsorption, ciprofloxacin, iron nanoparticles (Fe^0), nanocomposites, oxidation, titanium nanowires (TNWs)

HIGHLIGHTS

- Iron nanoparticles (Fe^0) were chemically deposited on titanium nanowires (TNWs).
- 20% was the optimum mass ratio between Fe0 and TNWs for efficient ciprofloxacin removal.
- The optimum dosage for ciprofloxacin removal by (20%-Fe0/TNW) composite was 1 g L^{-1}.
- Initial pH from 5 to 7 favoured the removal of ciprofloxacin by (20%-Fe^0/TNW) composite.
- 35 °C reaction temperature promoted the removal of ciprofloxacin from water.

INTRODUCTION

Over the years, pharmaceutical scientists have designed a broad spectrum of antibiotics to cure several bacterial infections in human and animals. Ciprofloxacin (CIP) is an extensively prescribed antibiotic worldwide to treat various infections, for instance, infections in bones, joints, skin, urinary tract, respiratory tract, as well as sexually transmitted infections; (Mao *et al.* 2019; Falyouna *et al.* 2022). The unwise and excessive application of CIP in human and veterinary medicine results in frequent detection of CIP and a wide range of other antibiotics in several water bodies (e.g., groundwater, lakes, rivers, etc.) across the universe with concentrations range from ng L^{-1} to mg L^{-1} (Yao *et al.* 2017). Residues of CIP get access to different compartments of the aquatic system through many routes. The most important route for CIP to enter the environment is the effluents of the traditional wastewater treatment plants (WWTPs). The unutilized amounts of CIP are being discharged from the treated bodies through urine and feces to reach the WWTPs (Boxall *et al.* 2012). Since it has been confirmed by several studies that WWTPs can't manage and efficiently remove the residues of CIP and their metabolites from the effluents,

they will eventually be evacuated with the treated wastewater to settle and contaminate the receiving water body (Yao *et al.* 2021). In addition, when the treated wastewater is used for irrigation or the WWTPs sludge is used as a fertilizer, residues of CIP can find their way to the groundwater through filtration and persist there for a long time (from months to years) (Archer *et al.* 2017). Furthermore, CIP can be introduced to the environment directly throughout the usage of CIP in the animal industry (e.g., aquaculture), or indirectly by using the manures of livestock as fertilizers in agriculture. Also, the effluents of CIP's manufacturing facilities and hospitals are possible routes to enter aquatic systems (Ji *et al.* 2021).

The persistent occurrence of CIP in water is linked to the accelerated growth of antimicrobial resistance genes (AMRs) in water (Rahdar *et al.* 2019; Mahmoud *et al.* 2021). These genes are famous in developing irremediable diseases. According to a review on the health consequences of AMRs, at least 700,000 persons are dying every year because of antimicrobial-resistant infections (O'Neill 2014). Also, the review speculated that this number is going to increase to more than 10 million by 2050 (O'Neill 2014). Thus, the development of an adequate and efficient technology to remove CIP from aqueous solutions is essential to protect lives and prevent the spread of such deadly genes in the limited water resources of earth.

Nanoscale zerovalent iron (Fe^0) is one of the most extensively applied nanomaterials to remediate different types of contaminated waters and to remove a broad spectrum of contaminants such as heavy metals, nutrients, radioactive elements, organic contaminants, and so on (Takami *et al.* 2019; Falyouna *et al.* 2020a; Maamoun *et al.* 2020a). Despite the superb characteristics of Fe^0 nanoparticles; for instance, high reactivity, high surface area, and multiple elimination mechanisms, they still have several drawbacks that restrict their ability to remediate antibiotics from water (Falyouna *et al.* 2019; Maamoun *et al.* 2021a). Fast surface oxidation, agglomeration and insignificant oxidation capacity are the main weaknesses of Fe^0 nanoparticles and various approaches were embraced to tackle these limitations (Mokete *et al.* 2020; Maamoun *et al.* 2021b). The previous researchers adopted numerous techniques to improve the performance of Fe^0 nanoparticles towards the elimination of CIP from water such as addition of Fenton reagent (i.e. hydrogen peroxide, persulfate, etc.), doping a noble metal on the surface of Fe^0 (i.e. Cu, Ni, Ag), and spreading of Fe^0 nanoparticles on a supporting material (i.e. biochar, graphene oxides, carbon nanotubes, etc.) (Chen *et al.* 2019; Pirsaheb *et al.* 2019; Falyouna *et al.* 2020b). Titanium oxide nanowires (TNWs) are an environmentally friendly, cost effective and excellent adsorbent and photocatalyst material for a variety of contaminants such as heavy metals (i.e. lead) and organics (i.e. phenol) (Youssef & Malhat 2014). The distinctive properties of TNWs, for instance, remarkable chemical stability, high photocatalysis and large surface area make them excellent supporting materials for Fe^0 nanoparticles (Yuan & Su 2004). This research aims to decorate the titanium nanowires (TNWs) with Fe^0 nanoparticles to decrease the aggregation of Fe^0 nanoparticles as well as supplement them with the photodegradation property in order to remove CIP from water.

MATERIALS AND METHODS

Materials

Ferric chloride hexahydrate ($FeCl_3.6H_2O$, JUNSEI, Japan), sodium borohydride (H_4BNa, Sigma Aldrich, USA), sodium hydroxide (NaOH, FUJIFILM Wako Pure Chemicals, Japan), and titanium (IV) oxide (TiO_2, FUJIFILM Wako Pure Chemicals, Japan) were utilized to synthesise Fe^0, TNWs and (Fe^0/TNW) nanocomposite. Ciprofloxacin hydrochloride monohydrate ($C_{17}H_{18}FN_3O_3{\cdot}HCl{\cdot}H_2O$, Tokyo Chemical Industry Co., Ltd, Japan) was dissolved in deionized water to prepare CIP solutions.

Synthesis of Fe^0 nanoparticles, TNWs, and (Fe^0/TNW) nanocomposites

A gram of Fe^0 nanoparticles was produced throughout the reduction of 92.49 mM of ferric chloride with 581.55 mM of sodium borohydride based on the previously reported steps in our articles (Maamoun *et al.* 2020b). Furthermore, titanium nanowires (TNWs) were synthesised by an alkaline hydrothermal process (Wang *et al.* 2018). In detail, 0.25 g of titanium (IV) oxide was totally dissolved in 40 mL of 10 M of sodium hydroxide solution. Then, the mixture was poured in a 150 mL Teflon-lined autoclave where the autoclave was tightly closed and placed inside an oven at 200 °C for one day. After the thermal treatment, the autoclave was taken out from the oven and left to cool down to room temperature. Afterwards, the acquired TNWs were collected by centrifugation and washed sequentially several times by 1% HCL, deionized water and ethanol until the pH of the solution reached 7. Finally, TNWs was dried at 65 °C for three days before being used in the

experiments. Moreover, (Fe^0/TNW) nanocomposites were synthesised in a similar way to synthesizing Fe^0 nanoparticles. For example, to produce 0.5 g of (Fe^0/TNW) with 50% mass ratio of TNW, 0.25 g of TNWs and 1.25 g of ferric chloride hexahydrate were mixed in 20 mL of ethanol for 10 min and ultrasonicated for 30 min before adding 50 mL of deoxygenated deionized water (DDIW) to prepare the 92.49 mM of ferric chloride solution. Then, the ferric ions (Fe^{3+}) were reduced to Fe^0 by the introduction of 581.55 mM of sodium borohydride under an anaerobic environment (Bensaida *et al.* 2020a). The final black precipitates were cleaned three times using 150 mL of DDIW during the vacuum filtration process.

Characterization of Fe^0 nanoparticles, TNWs, and (Fe^0/TNW) nanocomposites

The external morphology of Fe^0 nanoparticles, TNWs, and (Fe^0/TNW) nanocomposites was revealed by transmission electron microscopy (TEM, JEOL JEM-2100F). In addition, crystalline structure and chemical constituents of these materials were also obtained by conducting X-ray diffraction analysis (XRD, TTR Rigaku diffractometer).

Batch experiments

Batch experiments were conducted in 300 mL conical flasks and the conditions of the experiments were designed to be as follows: CIP initial concentration = 50 mg L^{-1}, volume of CIP solution = 200 mL, dosage of Fe^0, TNWs or (Fe^0/TNW) = 0.5 g L^{-1}, temperature = 25 °C, initial pH = 6 and contact time = 120 min. The reaction was started by placing the flask on a magnetic stirrer at 1,000 rpm and at specific time intervals (0, 5, 10, 15, 30, 60, 90, and 120 min), 2 mL liquid sample was withdrawn by a plastic syringe, filtered by 0.22 μm filter, and kept in 2 mL sampling tube for UV-Vis spectrophotometer analysis. The effect of TNWs mass ratio, (Fe^0/TNW) dosage, initial pH, and temperature was investigated in order to define the optimum removal conditions of CIP by (Fe^0/TNW) nanocomposites.

The performance of the materials was evaluated by calculating the removal efficiency using the following equation:

$$\text{Removal efficiency } (\%) = (C_0 - C_t)/C_0 \times 100\% \quad (1)$$

where, C_0 and C_t symbolise CIP initial concentration (mg L^{-1}) and CIP concentration at a given time t (mg L^{-1}), respectively.

Measurement of CIP concentration

CIP concentration was determined using a UV-vis spectrophotometer (UV-1280, Shimadzu, Japan) at a wavelength of 275 nm. The instrument was calibrated by using eight standard solutions of CIP, namely 0.25, 0.5, 0.75, 1, 2, 3, 4, and 5 mg L^{-1}. The constructed calibration curve is shown in Figure 1. The equation of the

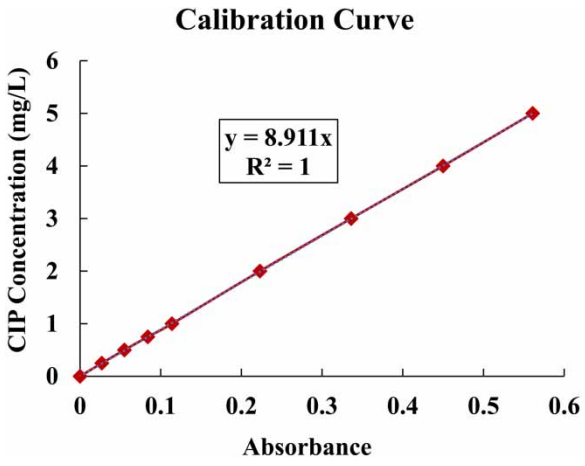

Figure 1 | Calibration curve of UV-1280.

calibration curve is as follows:

$$Y = 8.911X \quad (2)$$

where, Y and X represent CIP concentration (mg L^{-1}) and UV absorbance, respectively.

RESULTS AND DISCUSSION

Characterization of Fe^0 nanoparticles, TNWs, and (Fe^0/TNW) nanocomposites

TEM analysis was conducted to manifest the exterior morphology and size of Fe^0 nanoparticles, TNWs and (Fe^0/TNW) nanocomposite after the synthesis process. Figure 2(a) confirms that Fe^0 nanoparticles had a spherical shape with an approximate particle size of 56 nm and resorted to aggregate due to electrostatic and magnetic attractions between the nanoparticles. In addition, Figure 2(b) and 2(c) prove the formation of TNWs with a length of 8.46 μm and a width of 82.35 nm. Moreover, Figure 2(d) assures the successful deposition and dispersion of Fe^0 nanoparticles on the surface of TNWs. XRD technique was employed to reveal the crystalline structure of the materials mentioned in Figure 3. The XRD pattern of TNWs exhibited several strong and

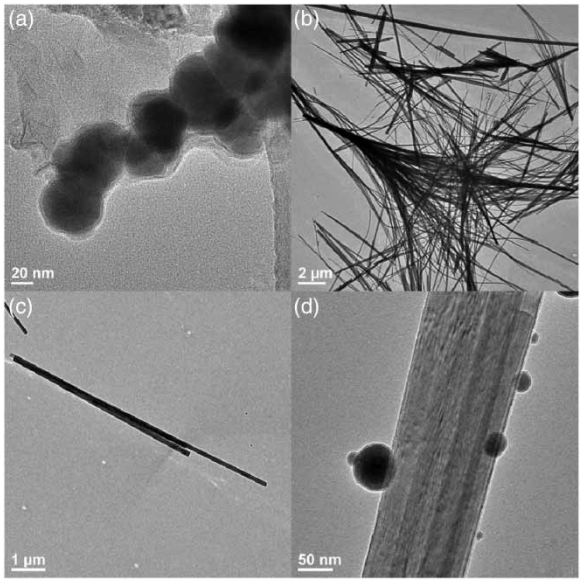

Figure 2 | TEM images for (a) Fe^0 nanoparticles, (b) & (c) TNWs, and (d) Fe^0/TNW nanocomposite.

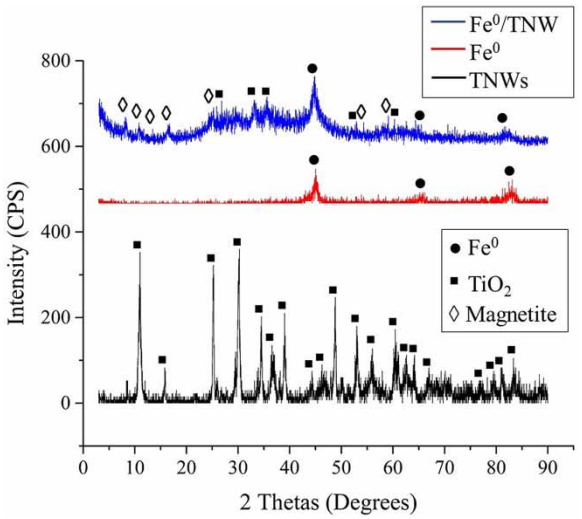

Figure 3 | XRD patterns for Fe^0 nanoparticles, TNWs, and Fe^0/TNW nanocomposite.

crystalline peaks named as titanium oxides (TiO_2) at different locations such as 11.13°, 25.20°, 30.26°, 48.84°, 64.18°, and 83.34° (Yuan & Su 2004). While, the three characteristic peaks of Fe^0 were identified in the XRD profile of Fe^0 nanoparticles at 44.45°, 65.15°, and 82.1° (Maamoun *et al.* 2019; Bensaida *et al.* 2020b). The XRD pattern of (Fe^0/TNW) nanocomposite demonstrates the presence of Fe^0 ($2\theta = 44.45°$, 65.15°, and 82.1°) and TiO_2 (29.45°, 33.14°, 35.6°, 52.92°, and 60.32°) peaks which evidences the successful fabrication of (Fe^0/TNW) nanocomposite.

Effect of TNWs mass ratio

Synthesis of (Fe^0/TNW) nanocomposites with different mass ratios of TNWs (5%, 10%, 20%, 30, 40, and 50%) was carried out in order to define the optimum mass ratio of TNWs that would overcome the limitations of Fe^0 nanoparticles, initiate the photodegradation of CIP, and attain a better CIP removal efficiency. Figure 4 summarizes the outputs of optimizing the TNW mass ratio. The removal efficiency of 50 mg L^{-1} of ciprofloxacin by 0.5 g L^{-1} of Fe^0 nanoparticles within the first 60 min was promising because it achieved 89.49%, as shown in Figure 4. However, at 90 min of reaction, the concentration of CIP in the aqueous solution started to increase, which proves the desorption of CIP molecules from the surface of Fe^0 nanoparticles. Afterwards, the performance of Fe^0 nanoparticles towards the removal of CIP severely deteriorated until it eventually reached 55.54% after 120 min of reaction. Similarly, it is clear from Figure 4 that the uptake behaviours of (Fe^0/TNW) nanocomposites with different percentages of TNWs and Fe^0 nanoparticles were almost identical as the (Fe^0/TNW) nanocomposites succeeded in removing significant proportion of CIP in the beginning of the reaction; nevertheless, desorption of CIP took place in the later stage of reaction. Fe^0/TNW nanocomposite with 20% TNW mass ratio exhibited a stable performance compared with other nanocomposites. This behaviour can be explained by the good dispersion and distribution of Fe^0 nanoparticles on the TNWs as presented in Figure 2(d), which decreased the aggregation, increased the surface area, and provided extra reactive sites for CIP removal. Thus, (20%-Fe^0/TNW) nanocomposite was selected to be used in the following experiments.

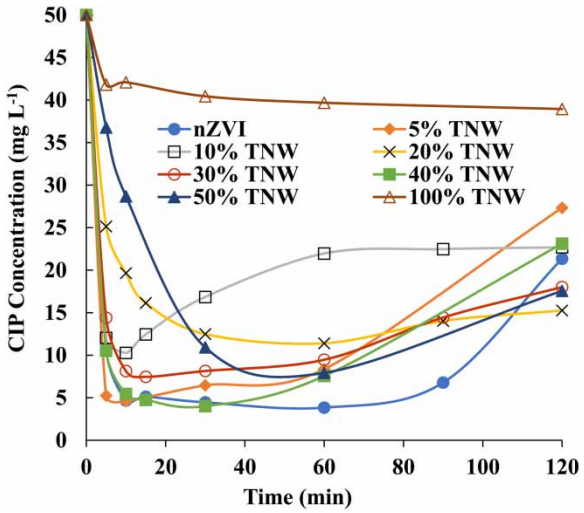

Figure 4 | Performance of Fe^0 and (Fe^0/TNW) nanocomposites with different ratios of TNWs. Removal conditions: CIP concentration: 50 mg L^{-1}, material dosage: 0.5 g L^{-1}, initial pH: 6, temperature: 25 °C, and contact time: 120 min.

Effect of (Fe^0/TNW) dosage

The dosage of (20%-Fe^0/TNW) nanocomposite was increased from 0.5 to 2 g L^{-1} to define the optimum dosage that could be applied in the treatment process. Figure 5 states that increasing the dosage of (20%-Fe^0/TNW) nanocomposite from 0.5 to 1 g L^{-1} significantly improved the elimination of CIP by approximately 30.28%. Doubling the dosage of (20%-Fe^0/TNW) nanocomposite provided additional adsorption locations for CIP as well as promoting the Fenton oxidation of CIP by generating more Fenton reagents (i.e. ferrous ions and hydrogen peroxide) and all these factors contributed to improve the removal of CIP (Shao *et al.* 2018). However, increasing the dosage to 1.5 and 2 g L^{-1} is not beneficial because they did not significantly enhance the removal of CIP. Therefore, based on the findings of Figure 5, the optimum dosage is 1 g L^{-1}.

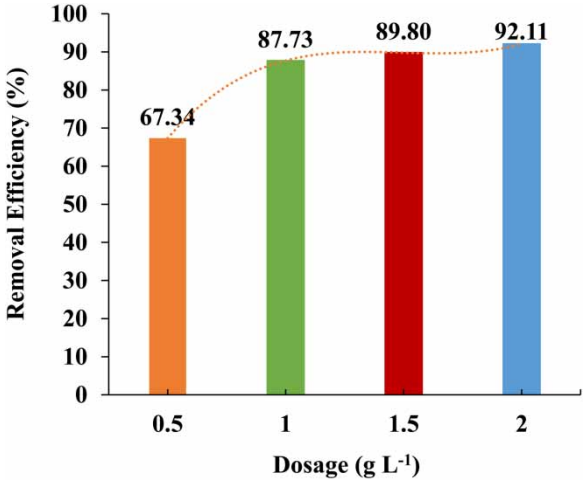

Figure 5 | Effect of (20%-Fe^0/TNW) nanocomposite dosage towards the removal of CIP. Removal conditions: CIP concentration: 50 mg L^{-1}, material dosage: (0.5–2) g L^{-1}, initial pH: 6, temperature: 25 °C, and contact time: 120 min.

Effect of initial pH

The influence of initial pH of the solution on the efficiency of (20%-Fe^0/TNW) nanocomposite was investigated by varying the initial pH from 5 to 11 as illustrated in Figure 6. At pH = 5, the nanocomposite was able to remove approximately 65.97% of 50 mg L^{-1} of CIP solution. This percentage trivially increased to 67.66% after increasing the initial pH to 7. Perini *et al.* reported that at pH 4.5 and 6.5, adsorption remarkably contributed to the total removal of CIP by zerovalent iron (ZVI) where the oxygen atoms of keto and carboxylic groups in the CIP structure formed bidentate complexes with the metals (de Lima Perini *et al.* 2014). On the other hand, the removal of CIP severely declined to 53.23% and 47.67 when the initial pH increased to 9 and 11, respectively. At the alkaline pH, the surface of Fe^0 nanoparticles will be covered by a layer of iron oxides, which may hide some reactive sites and hinder the possibility of adsorption of CIP (Liu *et al.* 2020). Hence, the preferable working range of pH for CIP removal by (20%-Fe^0/TNW) nanocomposite is from 5 to 7.

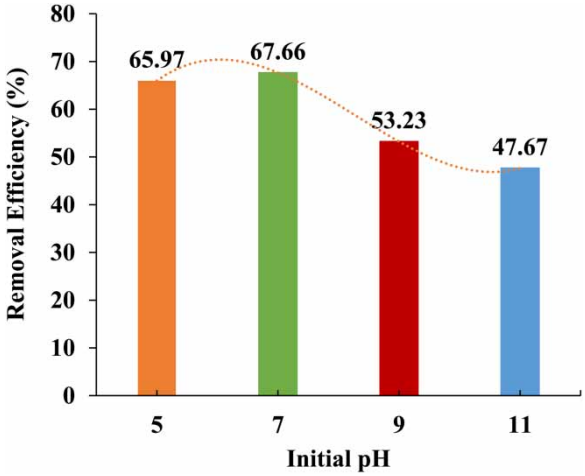

Figure 6 | Effect of initial pH of CIP solution on the performance of (20%-Fe^0/TNW) nanocomposite. Removal conditions: CIP concentration: 50 mg L^{-1}, material dosage: 0.5 g L^{-1}, initial pH: (5–11), temperature: 25 °C, and contact time: 120 min.

Effect of temperature

The impact of temperature on the removal of CIP by (20%-Fe^0/TNW) was observed by elevating the reaction temperature from 25 °C to 55 °C, as presented in Figure 7. 0.5 g L^{-1} of (20%-Fe^0/TNW) nanocomposite eliminated around 67.34% of 50 mg L^{-1} of CIP when the reaction temperature was set to 25 °C. Also, the removal

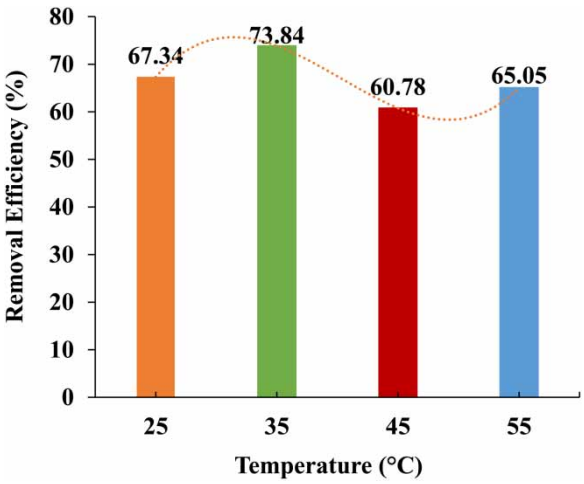

Figure 7 | Effect of reaction temperature on the removal efficiency of CIP by (20%-Fe^0/TNW) nanocomposite. Removal conditions: CIP concentration: 50 mg L^{-1}, material dosage: 0.5 g L^{-1}, initial pH: 6, temperature: (25–55) °C, and contact time: 120 min.

efficiency was further increased to 73.84% by increasing the temperature to 35 °C. This slight increase in the temperature may provide the necessary energy to facilitate the adsorption of CIP by (20%-Fe^0/TNW) nanocomposite (Chen *et al.* 2019). Conversely, incrementing the temperature to 45 °C and 55 °C resulted in declining removal efficiency to 60.78% and 65.05%, respectively. These outcomes are in a good agreement with results of Zhang *et al.* when they remediated norfloxacin from aqueous solution using nZVI/H_2O_2 system (Zhang *et al.* 2017).

Comparison between the performance of (Fe^0/TNW) nanocomposite and other reported materials in removing CIP from water

Table 1 demonstrates a comparison between (Fe^0/TNW) nanocomposite and some of the recently reported materials in the literature in terms of CIP removal from water. While constructing Table 1, CIP initial concentration was taken into consideration to perform a fair comparison between the materials. According to Table 1, (Fe^0/TNW) nanocomposite exhibited a superior removal capacity of CIP (99.64 mg g^{-1}) compared with the removal capacities of other materials. This comparison proves the potential of using (Fe^0/TNW) nanocomposite in remediating CIP-contaminated water.

Table 1 | Comparison between (Fe^0/TNW) nanocomposite and other reported materials in ciprofloxacin removal from water

Material name	Maximum removal capacity (mg g^{-1})	References
20%-Fe^0/TNW nanocomposite	99.64	This study
Sugarcane bagasse	13.6	Peñafiel *et al.* (2021)
Magnetic Fe_3O_4–MoO_3-AC nanocomposite	45	Mahmoud *et al.* (2021)
Sodium intercalated Ti_3C_2Tx (SI-$Ti_3C_2T_x$) MXene nanosheets	65	Ghani *et al.* (2021)
Silica xerogels	24.45	Guzel Kaya *et al.* (2021)
KOH modified biochar derived from potato stems and leaves	23.36	Li *et al.* (2017)
Magnetic carbon composite (Fe_3O_4/C)	90.1	Mao *et al.* (2016)
Magnetic sludge biochar (Fe/Zn-SBC)	74.2	Ma *et al.* (2021)

CONCLUSIONS

This research project investigated the performance of (Fe^0/TNW) nanocomposites towards the removal of ciprofloxacin (CIP) from water. TEM and XRD analysis were carried out to reveal the morphological characteristics as well as the crystalline structure of Fe^0 nanoparticles, titanium nanowires (TNWs), and (Fe^0/TNW) nanocomposites. The TEM results proved the successful synthesis of the chain-like structure Fe^0 nanoparticles and TNWs. Moreover,

the TEM images confirmed the deposition and distribution of Fe^0 nanoparticles on the surface of TNWs. Furthermore, the outcomes of XRD analysis supported the findings of TEM and evidenced the successful formation of Fe^0 nanoparticles, TNWs, and (Fe^0/TNW) nanocomposite. Several batch experiments were also performed to illustrate the optimum mass proportion of TNWs (5, 10, 20, 30, 40, and 50%) in (Fe^0/TNW) in the nanocomposite to achieve the best removal efficiency of CIP from water. The optimum percentage of TNWs in the prepared (Fe^0/TNW) nanocomposites was 20% as it exhibited a stable performance with a minimal desorption behaviour (67.34% after 120 min) compared with the other percentages. In addition, another set of batch experiments was conducted to disclose the optimum removal conditions of CIP by the (20%-Fe^0/TNW) nanocomposite such as dosage, initial pH and temperature. The results of these experiments concluded that 50 mg L^{-1} of CIP was optimally removed by 1 g L^{-1} of (20%-Fe^0/TNW) nanocomposite at initial pH of 7 and under 35 °C.

DATA AVAILABILITY STATEMENT

All relevant data are included in the paper or its Supplementary Information.

REFERENCES

Archer, E., Petrie, B., Kasprzyk-Hordern, B. & Wolfaardt, G. M. 2017 The fate of pharmaceuticals and personal care products (PPCPs), endocrine disrupting contaminants (EDCs), metabolites and illicit drugs in a WWTW and environmental waters. *Chemosphere* **174**, 437–446. https://doi.org/10.1016/j.chemosphere.2017.01.101.

Bensaida, K., Eljamal, R., Kareman, E., Sughihara, Y. & Eljamal, O. 2020a The impact of iron bimetallic nanoparticles on bulk microbial growth in wastewater. *Journal of Water Process Engineering* **40**, 101825. https://doi.org/10.1016/j.jwpe.2020.101825.

Bensaida, K., Maamoun, I., Eljamal, R., Falyouna, O., Sugihara, Y. & Eljamal, O. 2020b *Enhancement of Power Generation in Microbial Fuel Cells (Mfcs) Using Iron/Copper Nanoparticles*. The 6th IEICES-2020, Kyushu University, Fukuoka, Japan.

Boxall, A. B. A., Rudd, M. A., Brooks, B. W., Caldwell, D. J., Choi, K., Hickmann, S., Innes, E., Ostapyk, K., Staveley, J. P. & Verslycke, T. 2012 Pharmaceuticals and personal care products in the environment: what are the big questions? *Environmental Health Perspectives* **120**(9), 1221–1229.

Chen, L., Yuan, T., Ni, R., Yue, Q. & Gao, B. 2019 Multivariate optimization of ciprofloxacin removal by polyvinylpyrrolidone stabilized NZVI/Cu bimetallic particles. *Chemical Engineering Journal* **365**, 183–192. https://doi.org/10.1016/j.cej.2019.02.051.

de Lima Perini, J. A., Silva, B. F. & Nogueira, R. F. P. 2014 Zero-valent iron mediated degradation of ciprofloxacin – assessment of adsorption, operational parameters and degradation products. *Chemosphere* **117**, 345–352. https://doi.org/10.1016/j.chemosphere.2014.07.071.

Falyouna, O., Eljamal, O. & Maamoun, I. 2019 Removal of cesium from contaminated waters by employing iron-based nanoparticles and nanocomposites. In: *The 5th International Exchange and Innovation Conference on Engineering & Sciences (IEICES)* (5, Pp. 26–27). Interdisciplinary Graduate School of Engineering Sciences, Kyushu University, Fukuoka, Japan.

Falyouna, O., Eljamal, O., Maamoun, I., Tahara, A. & Sugihara, Y. 2020a Magnetic zeolite synthesis for efficient removal of cesium in a lab-scale continuous treatment system. *Journal of Colloid and Interface Science* **571**. https://doi.org/10.1016/j.jcis.2020.03.028

Falyouna, O., Maamoun, I., Bensaida, K., Sugihara, Y. & Eljamal, O. 2020b Removal of ciprofloxacin from aqueous solutions by nanoscale zerovalent iron-based materials: a mini review. *Proceedings of International Exchange and Innovation Conference on Engineering & Sciences (IEICES)* **6**, 179–185. https://doi.org/10.5109/4102485.

Falyouna, O., Maamoun, I., Bensaida, K., Tahara, A., Sugihara, Y. & Eljamal, O. 2022 Encapsulation of iron nanoparticles with magnesium hydroxide shell for remarkable removal of ciprofloxacin from contaminated water. *Journal of Colloid and Interface Science* **605**, 813–827. https://doi.org/10.1016/j.jcis.2021.07.154.

Ghani, A. A., Shahzad, A., Moztahida, M., Tahir, K., Jeon, H., Kim, B. & Lee, D. S. 2021 Adsorption and electrochemical regeneration of intercalated $Ti_3C_2T_x$ MXene for the removal of ciprofloxacin from wastewater. *Chemical Engineering Journal* **421**, 127780. https://doi.org/10.1016/j.cej.2020.127780.

Guzel Kaya, G., Aznar, E., Deveci, H. & Martínez-Máñez, R. 2021 Low-cost silica xerogels as potential adsorbents for ciprofloxacin removal. *Sustainable Chemistry and Pharmacy* **22**, 100483. https://doi.org/10.1016/j.scp.2021.100483.

Ji, H., Wang, T., Huang, T., Lai, B. & Liu, W. 2021 Adsorptive removal of ciprofloxacin with different dissociated species onto titanate nanotubes. *Journal of Cleaner Production* **278**, 123924. https://doi.org/10.1016/j.jclepro.2020.123924.

Li, R., Wang, Z., Guo, J., Li, Y., Zhang, H., Zhu, J. & Xie, X. 2017 Enhanced adsorption of ciprofloxacin by KOH modified biochar derived from potato stems and leaves. *Water Science and Technology* **77**(4), 1127–1136. https://doi.org/10.2166/wst.2017.636.

Liu, J., Du, Y., Sun, W., Chang, Q. & Peng, C. 2020 A granular adsorbent-supported Fe/Ni nanoparticles activating persulfate system for simultaneous adsorption and degradation of ciprofloxacin. *Chinese Journal of Chemical Engineering* **28**(4), 1077–1084. https://doi.org/10.1016/j.cjche.2019.12.019.

Ma, Y., Li, M., Li, P., Yang, L., Wu, L., Gao, F., Qi, X. & Zhang, Z. 2021 Hydrothermal synthesis of magnetic sludge biochar for tetracycline and ciprofloxacin adsorptive removal. *Bioresource Technology* **319**, 124199. https://doi.org/10.1016/j.biortech.2020.124199.

Maamoun, I., Eljamal, O., Thompson, I., Eljamal, R., Falyouna, O. & Sugihara, Y. 2019 Effect of nano zero valent iron delivery method into porous media on phosphorus removal from groundwater. *Proceedings of International Exchange and Innovation Conference on Engineering & Sciences (IEICES)* **5**(October), 9–11.

Maamoun, I., Eljamal, O., Falyouna, O., Eljamal, R. & Sugihara, Y. 2020a Multi-objective optimization of permeable reactive barrier design for Cr(VI) removal from groundwater. *Ecotoxicology and Environmental Safety* **200**. https://doi.org/10.1016/j.ecoenv.2020.110773

Maamoun, I., Eljamal, O., Falyouna, O., Eljamal, R. & Sugihara, Y. 2020b Stimulating effect of magnesium hydroxide on aqueous characteristics of iron nanocomposites. *Water Science and Technology* **80**(10), 1996–2002. https://doi.org/10.2166/wst.2020.027.

Maamoun, I., Eljamal, R., Falyouna, O., Bensaida, K., Sugihara, Y. & Eljamal, O. 2021a Insights into kinetics, isotherms and thermodynamics of phosphorus sorption onto nanoscale zero-valent iron. *Journal of Molecular Liquids* **328**, 115402. https://doi.org/10.1016/j.molliq.2021.115402.

Maamoun, I., Falyouna, O., Eljamal, R., Bensaida, K. & Eljamal, O. 2021b Optimization modeling of nFe0/Cu-PRB design for Cr (VI) removal from groundwater. *International Journal of Environmental Science and Development* **12**, 131–138.

Mahmoud, M. E., Saad, S. R., El-Ghanam, A. M. & Mohamed, R. H. A. 2021 Developed magnetic Fe_3O_4–MoO_3-AC nanocomposite for effective removal of ciprofloxacin from water. *Materials Chemistry and Physics* **257**, 123454. https://doi.org/10.1016/j.matchemphys.2020.123454.

Mao, H., Wang, S., Lin, J.-Y., Wang, Z. & Ren, J. 2016 Modification of a magnetic carbon composite for ciprofloxacin adsorption. *Journal of Environmental Sciences* **49**, 179–188.

Mao, Q., Zhou, Y., Yang, Y., Zhang, J., Liang, L., Wang, H., Luo, S., Luo, L., Jeyakumar, P., Ok, Y. S. & Rizwan, M. 2019 Experimental and theoretical aspects of biochar-supported nanoscale zero-valent iron activating H_2O_2 for ciprofloxacin removal from aqueous solution. *Journal of Hazardous Materials* **380**, 120848. https://doi.org/10.1016/j.jhazmat.2019.120848.

Mokete, R., Eljamal, O. & Sugihara, Y. 2020 Exploration of the reactivity of nanoscale zero-valent iron (NZVI) associated nanoparticles in diverse experimental conditions. *Chemical Engineering and Processing – Process Intensification* **150**, 107879. https://doi.org/10.1016/j.cep.2020.107879.

O'Neill, J. 2014 *Antimicrobial Resistance: Tackling A Crisis for the Health and Wealth of Nations*. Review on Antimicrobial Resistance.

Peñafiel, M. E., Matesanz, J. M., Vanegas, E., Bermejo, D., Mosteo, R. & Ormad, M. P. 2021 Comparative adsorption of ciprofloxacin on sugarcane bagasse from Ecuador and on commercial powdered activated carbon. *Science of The Total Environment* **750**, 141498. https://doi.org/10.1016/j.scitotenv.2020.141498.

Pirsaheb, M., Moradi, S., Shahlaei, M., Wang, X. & Farhadian, N. 2019 Simultaneously implement of both weak magnetic field and aeration for ciprofloxacin removal by Fenton-like reaction. *Journal of Environmental Management* **246**, 776–784.

Rahdar, S., Rahdar, A., Igwegbe, C. A., Moghaddam, F. & Ahmadi, S. 2019 Synthesis and physical characterization of nickel oxide nanoparticles and its application study in the removal of ciprofloxacin from contaminated water by adsorption: equilibrium and kinetic studies. *Desalination and Water Treatment* **141**, 386–393.

Shao, Y., Zhao, P., Yue, Q., Wu, Y., Gao, B. & Kong, W. 2018 Preparation of wheat straw-supported Nanoscale Zero-Valent Iron and its removal performance on ciprofloxacin. *Ecotoxicology and Environmental Safety* **158**, 100–107. https://doi.org/10.1016/j.ecoenv.2018.04.020.

Takami, S., Eljamal, O., Khalil, A. M. E., Eljamal, R. & Matsunaga, N. 2019 Development of continuous system based on nanoscale zero valent iron particles for phosphorus removal. *Journal of JSCE* **7**(1), 30–42. https://doi.org/10.2208/journalofjsce.7.1_30.

Wang, X., Wang, A., Lu, M. & Ma, J. 2018 Synthesis of magnetically recoverable Fe0/graphene-TiO_2 nanowires composite for both reduction and photocatalytic oxidation of metronidazole. *Chemical Engineering Journal* **337**, 372–384.

Yao, L., Wang, Y., Tong, L., Deng, Y., Li, Y., Gan, Y., Guo, W., Dong, C., Duan, Y. & Zhao, K. 2017 Occurrence and risk assessment of antibiotics in surface water and groundwater from different depths of aquifers: a case study at Jianghan Plain, central China. *Ecotoxicology and Environmental Safety* **135**, 236–242. https://doi.org/10.1016/j.ecoenv.2016.10.006.

Yao, B., Luo, Z., Yang, J., Zhi, D. & Zhou, Y. 2021 FeIIFeIII layered double hydroxide modified carbon felt cathode for removal of ciprofloxacin in electro-Fenton process. *Environmental Research* **197**, 111144. https://doi.org/10.1016/j.envres.2021.111144.

Youssef, A. M. & Malhat, F. M. 2014 Selective removal of heavy metals from drinking water using titanium dioxide nanowire. *Macromolecular Symposia* **337**(1), 96–101. https://doi.org/10.1002/masy.201450311.

Yuan, Z. Y. & Su, B. L. 2004 Titanium oxide nanotubes, nanofibers and nanowires. *Colloids and Surfaces A: Physicochemical and Engineering Aspects* **241**(1–3), 173–183. https://doi.org/10.1016/j.colsurfa.2004.04.030.

Zhang, W., Gao, H., He, J., Yang, P., Wang, D., Ma, T., Xia, H. & Xu, X. 2017 Removal of norfloxacin using coupled synthesized nanoscale zero-valent iron (nZVI) with H_2O_2 system: optimization of operating conditions and degradation pathway. *Separation and Purification Technology* **172**, 158–167. https://doi.org/10.1016/j.seppur.2016.08.008.

First received 13 July 2021; accepted in revised form 7 September 2021. Available online 21 September 2021